Journal of Materials Chemistry C

ROYAL SOCIETY OF CHEMISTRY

PAPER

View Article Online
View Journal | View Issue

Cite this: J. Mater. Chem. C, 2023, 11, 11486

Manipulating the transition of aggregated states to control the photochromism in a new triphenylethylene derivative†

Mingyao Shen,[a] Cheng Huang,[a] Yuxin Xiao,[a] Rongjuan Huang,[a] Vonika Ka-Man Au *[b] and Tao Yu *[a]

Received 29th March 2023,
Accepted 8th August 2023

DOI: 10.1039/d3tc01093g

rsc.li/materials-c

Revealing the differences between crystalline and amorphous states in solid samples can both deepen the understanding of their structure–property relationships and promote the development of versatile materials based on the same compounds. Herein, we report a new triphenylethylene derivative that exhibits different photochromic properties in two aggregated states. The further characterization studies showed that the photochromism was associated with a transition from the crystalline to amorphous state. Moreover, the two aggregated states of samples can be readily interconverted into each other and applied to convertible information storage. This work provides a strategy for controlling photochromism by manipulating the transition of aggregated states, paving a new way for the regulation of photochromism.

1. Introduction

Photoresponsive materials are a class of smart materials that can exhibit various responsive behaviors (*e.g.* changes in color,[1–3] shape[4–6] and refractive index[7]) in response to external light stimuli. Among the diverse responsive behaviors, photochromism is one of the most fascinating properties due to the reversible transformation of chemical structures with corresponding color changes under photoirradiation.[8–10] Since Fritzsche[11] first reported the photochromic phenomena of a solution of tetracene in 1867, the field of photochromism has seen great developments with broad applications in optical switches,[12–14] information encryption[15–19] and memory storage systems.[20–22]

In the past several decades, organic photochromic materials have attracted tremendous attention and several photochromic systems have gradually emerged, including azobenzenes,[23–25] spiropyrans,[26–29] fulgides,[30–33] diarylethylenes[34–37] and their derivatives. Restricted by the complex synthetic process, poor thermal stability, and weak fatigue resistance to varying degrees, these materials, however, are facing challenges in widespread practical applications. Thus, a new organic photochromic system with fast response is urgently needed. Recently, triphenylethylene derivatives are expected to become a new type of organic photochromic molecules owing to their simple synthesis, facile modifiability, and diverse properties. In 2016, Yu and co-workers[38] first reported the photochromism of dichloro-substituted triphenylethylene derivatives, whose color changed from white to red with a concomitant quenching in its

[a] Frontiers Science Center for Flexible Electronics (FSCFE), Shaanxi Institute of Flexible Electronics (SIFE) & Shaanxi Institute of Biomedical Materials and Engineering (SIBME), Northwestern Polytechnical University (NPU), 127 West Youyi Road, Xi'an 710072, China. E-mail: iamtyu@nwpu.edu.cn

[b] Department of Science and Environmental Studies, The Education University of Hong Kong, 10 Lo Ping Road, Tai Po, New Territories, Hong Kong, China. E-mail: kmau@eduhk.hk

† Electronic supplementary information (ESI) available: Synthetic procedures, experimental details, and supplemental figures. See DOI: https://doi.org/10.1039/d3tc01093g

Tao Yu

Tao Yu received his PhD degree from the University of Hong Kong and carried out postdoctoral studies under the supervison of Professor Vivian W.-W. Yam. In 2015, he moved to Sun Yat-Sen University as Associate Professor. In 2018, he obtained his current professor position in Northwestern Polytechnical University. His research interests focus on organic optoelectronic functional materials such as photochromic materials, mechanoluminescent materials and phosphorescent materials.

blue emission upon UV irradiation (365 nm). The color and fluorescence could return to their original state after stopping the illumination for several seconds. After spin-coating a dichloromethane solution of the compounds onto a SiO_2 substrate and removing the solvent by evaporation, the obtained microcrystalline surfaces showed different morphologies and wettability in the presence and absence of UV irradiation. The surface of the microcrystals before UV illumination was rod-shaped; while the surface became scale-like and the wettability reduced drastically upon the irradiation of UV light, exhibiting the combination of photochromic and photoresponsive wettability properties. From then on, Yu's group has successively explored the diverse properties of triarylethylene derivatives, including morphology-dependent photochromism,[39] real-time photo-controlled surface,[40] oxidation gated photochromism,[41] and photochromic-photoluminescent dual-mode response.[42] Very recently, Yu and coworkers[43] have prepared a new photo-responsive material, a methylmethacrylate-containing triphenylethylene ($TrPEF_2$-MA), that can be directly used for digital light processing (DLP) 3D printing. $TrPEF_2$-MA-printed 3D structures have excellent photochromic properties such as high resolution (50 μm), fast photo-response, and good reversibility. The saturation chromaticity of the 3D structures can also be accurately controlled by adjusting the ratio of $TrPEF_2$ and MA in the component. Moreover, through DLP-3D printing, the materials can realize information encryption and storage characteristics in 3D structures, which has a good application prospect.

The aggregated state of photochromic molecules plays an important role in controlling the optical and photochromic properties. To date, photochromism of triphenylethylene derivatives that have been reported typically occurs in solution states or polymer thin films instead of crystalline states, owing to the difficulty of photocyclization occurring in the rigid crystalline environment. However, it is crucial to develop solid-state photochromic materials for practical applications. The transformation of the aggregated state of solid powder is expected to have an impact on the regulation of photochromic properties.

Herein, a new triphenylethylene derivative, (2-(2,2-bis(4-fluorophenyl)vinyl)phenyl)diphenylphosphine oxide (TrPE*o*PO), was designed and synthesized. Initially, the crystalline powders obtained from slow recrystallization showed no obvious photochromism. However, the amorphous state of the same compound obtained from rapid vacuum rotary evaporation showed excellent photochromic properties and recyclability. Moreover, the different aggregated states and photochromic properties can be interconverted into each other. Therefore, we successfully realized the gated transformation of photochromism by switching the aggregated state of the solid from the crystalline to the amorphous form, demonstrating a new strategy for the regulation of photochromism.

2. Results and discussion

2.1. Photophysical and photochromic properties

The simplified synthetic route to TrPE*o*PO is shown in Fig. 1a, whereas the detailed synthetic procedure can be found in the supplementary information (ESI†). The chemical structure and purity of TrPE*o*PO were characterized by NMR spectroscopy, and high-resolution EI mass spectrometry (Fig. S1–S3, ESI†).

The basic photophysical properties of TrPE*o*PO were first studied in the solution state. As shown in Fig. 1b, the UV-vis absorption and photoluminescence (PL) spectra of TrPE*o*PO were recorded in diluted dichloromethane (DCM, c = 1.0 × 10^{-5} M) at room temperature. There was an absorption band with a maximum at *ca.* 315 nm, which could be attributed to the π–π* transition of TrPE*o*PO according to the previous reports with similar structures.[44] In the PL spectra, the

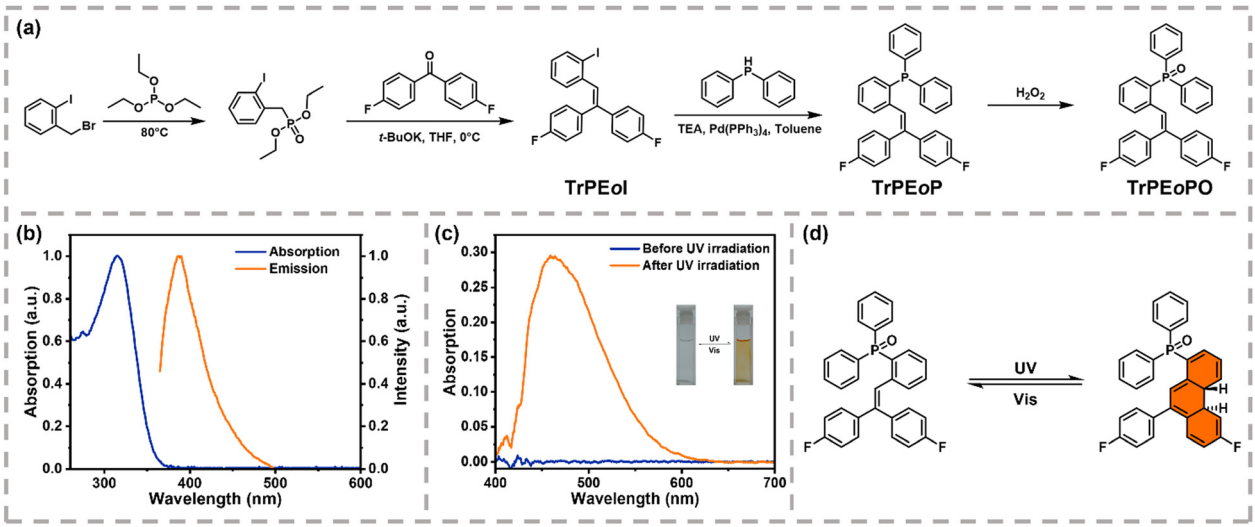

Fig. 1 (a) Synthetic routes to the target compound, TrPE*o*PO (THF: tetrahydrofuran; TEA: triethylamine). (b) UV-vis absorption and emission spectra of TrPE*o*PO (c = 1.0 × 10^{-5} M) in dichloromethane. (c) UV-Vis absorption spectra of TrPE*o*PO (c = 0.10 M) in dichloromethane before and after the irradiation of UV light (365 nm). Inset: images showing the photochromism of TrPE*o*PO in dichloromethane under daylight before and after UV irradiation. (d) Schematic diagram of the photochromic mechanism of TrPE*o*PO.

TrPE*o*PO in DCM showed an emission peak at 387 nm, which was consistent with its violet emission upon excitation with UV light (365 nm).

Furthermore, the photochromic properties of TrPE*o*PO were also investigated in DCM solution (c = 0.10 M). Upon UV light irradiation (365 nm), the colorless and transparent solution turned orange gradually and a new absorption band with a maximum at 460 nm was observed for TrPE*o*PO (Fig. 1c). Meanwhile, the absorption peak disappeared slowly along the decolorization of the solution from orange to the original colorless state when exposed to visible light or when the UV irradiation (365 nm) was removed for about 30 minutes. According to the previous work,[38] the reversible changes in color can be ascribed to the ring-closure and ring-opening of the stilbene moiety of TrPE*o*PO as illustrated in Fig. 1d. As a result, the degree of conjugation of the molecular structure was changed, thereby realizing the displacement of its absorption spectrum.

In contrast to the photochromism in the solution state, the white solid powders obtained directly by recrystallization from a solution of TrPE*o*PO in DCM/hexane (1 : 1 v/v) showed no photochromic phenomenon when viewed with naked eyes. Nevertheless, upon the removal of the solvent by rapid vacuum rotary evaporation, amorphous samples can be obtained. After quickly cooling down to the room temperature, the amorphous samples with glossy surfaces unexpectedly exhibited photochromic properties. Upon UV light irradiation (365 nm) for 10 seconds, the samples could change their appearance from colorless to orange (Fig. 2a).

Time-dependent UV-vis reflectance spectroscopic studies were carried out as shown in Fig. 2b–e. In contrast to the weak rise of the intensity of the absorption band for the crystalline powder, the amorphous form of TrPE*o*PO exhibited an obvious and significant enhancement in the absorbance at 500 nm. After irradiation for about 150 s, the increase in absorbance stopped. Similar to the aggregated-state-dependent irradiation spectrum described above, although UV light (365 nm) was irradiated for over 3 minutes, there was no obvious absorption peak in the reflectance spectra of TrPE*o*PO in the crystalline state (Fig. 2d). The intensity of the absorption band (peak at 500 nm) gradually decreased with the removal of the UV light (365 nm) and returned to its initial colorless state in 3600 seconds in the dark as shown in Fig. 2e. Moreover, the photochromic bleaching rates and half-lives of TrPE*o*PO in solution and amorphous states were calculated by the first-order rate equation as shown in Fig. S4 (ESI†). In addition, the amorphous state of TrPE*o*PO exhibited excellent recyclability during the photochromic process. As depicted in Fig. 2f, the sample showed no detectable fatigue even after 20 cycles of photochromic and bleaching. The high recyclability indicates its potential applications as rewritable and optical information storage materials.

2.2. Mechanism investigation of the distinct properties

In addition to the large difference in the photochromic properties, there were also distinctions in the luminescence properties of TrPE*o*PO in crystalline and amorphous states (Fig. 3a). As shown in Fig. 3b, the emission peaks of crystalline powders were located at 378 nm and 395 nm. However, the emission band of the amorphous powder appeared at 422 nm and the red shift was *ca.* 4×10^5 cm^{-1}. As it is uncommon for such a large peak displacement to occur in the visible region of the high-energy zone, this shift is probably due to the effect of molecular

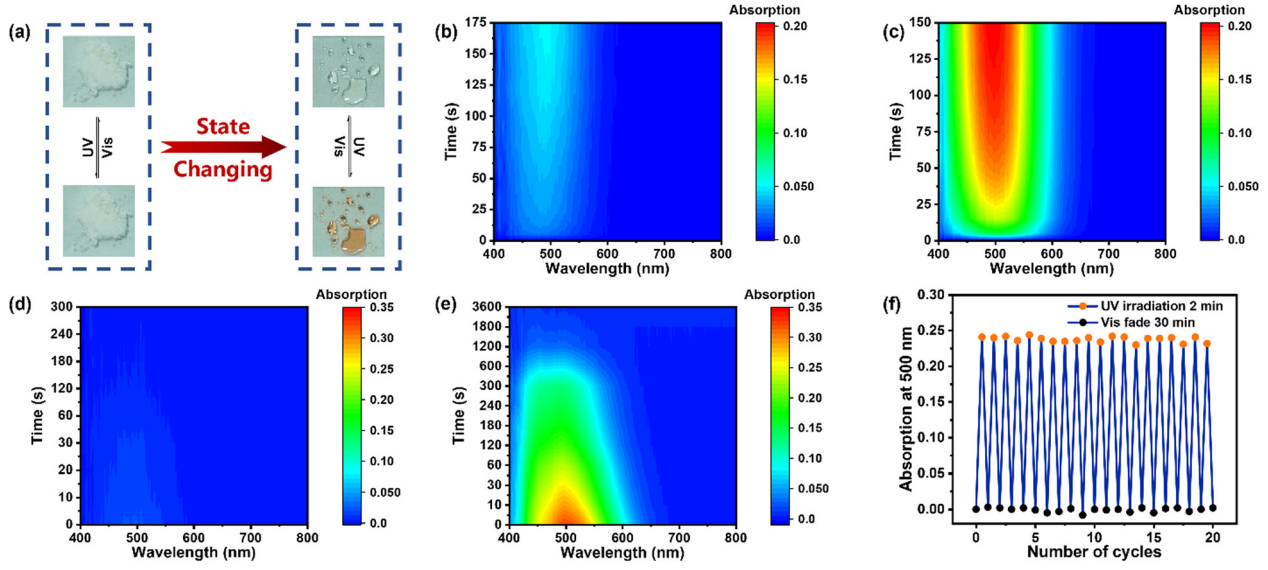

Fig. 2 (a) Images showing the photochromism of TrPE*o*PO before (the left) and after (the right) state transformation. Time dependent UV-vis reflectance spectra of TrPE*o*PO before (b) and after (c) state transformation during the photochromic irradiation process. Time dependent UV-vis reflectance spectra of TrPE*o*PO before (d) and after (e) state transformation during the photochromic bleaching process. (f) Recycling of the photochromic process of TrPE*o*PO after state transformation as a function of exposure to UV light (365 nm) and visible light for 2 minutes and 30 minutes, respectively.

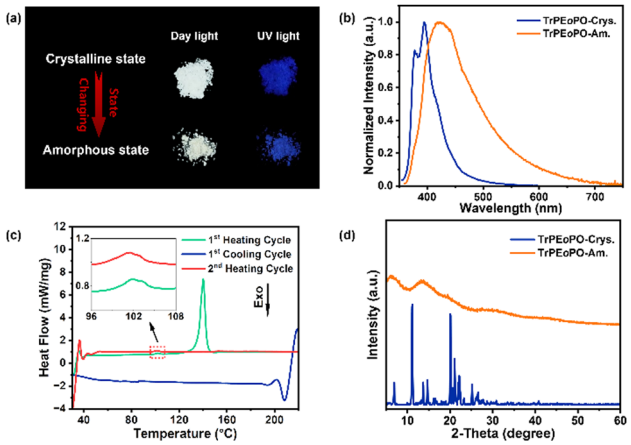

Fig. 3 (a) Images of the crystalline and amorphous TrPEoPO powders under daylight and the irradiation of UV light. (b) The PL spectra of TrPEoPO in the crystalline and amorphous states. (c) DSC curves of TrPEoPO. (d) PXRD pattern of TrPEoPO.

accumulation on both states. The corresponding fluorescence lifetime is detailed in Table S1 (ESI†).

Thermogravimetric analysis (TGA) was carried out to monitor the weight loss of TrPE*o*PO under an atmosphere of N_2 at different temperatures. As can be seen in Fig. S5 (ESI†), there was only one mass loss process with no residue, which ended at about 390 °C. Meanwhile, the decomposition temperature (T_d), defined as the temperature with a 5% loss in weight, of TrPE*o*PO was 283 °C. The relatively high T_d indicated the good thermal stability of the samples, which was attributable to the rigid structure comprised of the triphenylethylene and phosphine oxy groups of TrPE*o*PO. Second, Fig. 3c shows the differential scanning calorimetry (DSC) curves of TrPE*o*PO. Initially, the crystalline samples were heated from 30 to 220 °C to eliminate the thermal history with a heating rate of 10 °C min^{-1} under a N_2 atmosphere. An endothermic peak due to melting could be obviously observed at 136 °C. Then the amorphous powders were rapidly cooled back to 30 °C for the second cycle of DSC analysis. When the cooled samples were reheated at the same heating rate, a clear shift in the heat capacity was observed. The glass transition temperature (T_g) was determined from the outset of heat flow to be 95 °C. The emergence of the glass transition phenomenon, which is considered as one of the characteristics of amorphous systems, suggested the formation of the amorphous samples after melting and cooling. In addition, the above conclusion can be further verified by the characterization *via* PXRD. The PXRD patterns of TrPE*o*PO in the two aggregated states are shown in Fig. 3d. Initially, the crystalline powders exhibited clear diffraction peaks evidencing a high crystallinity, which is consistent with the presence of a high endothermic peak in the first heating cycle in the DSC curve as described above. However, the samples obtained from rapid vacuum rotary evaporation showed only diffuse scattering rather than sharp diffraction peaks, indicating the formation of an amorphous state.

The transition of the aggregated states implies the collapse of the rigid environment and the weakening of the intermolecular interactions, in turn facilitating the occurrence of the ring-closure reaction of TrPE*o*PO under UV light (365 nm). This is the fundamental reason why the same sample exhibits distinct luminescent and photochromic properties after the transformation from a crystalline aggregated state to an amorphous aggregated state.

2.3. Photocontrolled patterning applications

Based on the distinct photochromic properties of the crystalline and amorphous forms of TrPE*o*PO, they could be selectively used in potential applications such as optical recording, optical switching, and displays. As depicted in Fig. 4a, the significantly different photocontrolled patterning properties of crystalline and amorphous powders of TrPE*o*PO were demonstrated.

As shown in Fig. 4b, the crystalline samples of TrPE*o*PO were placed on a quartz plate (30 × 30 × 3 mm), in the center of which was a groove with a side length of 20 mm and a thickness of 2 mm. Clearly, the white crystalline powders of TrPE*o*PO showed no photochromism and remained unchanged under UV light (365 nm), neither with nor without photo masks. After UV irradiation, however, the amorphous solid with a transparent and smooth surface showed the shape of a flower and turned orange quickly under the cover by black mask A, due to the photochromism of TrPE*o*PO. When the mask was removed and treated with visible light, the orange color disappeared

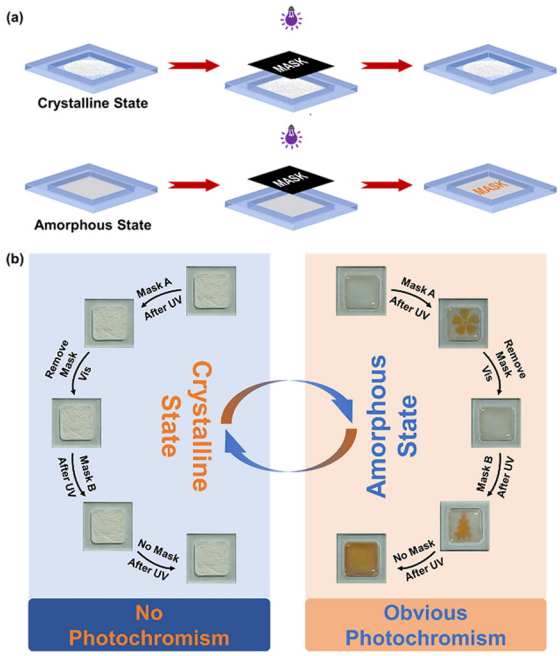

Fig. 4 (a) Schematic representation of the photo-controlled patterning applications of the crystalline and amorphous sample in a quartz plate with groove. (b) Consecutive demonstrations of printing on the crystalline and amorphous TrPEoPO sample by masking method. (Mask A and Mask B were made with black hollowed-out photo masks of a flower and a tower, respectively).

gradually and the initial colorless state was recovered. Additional patterns such as a tower could then be consecutively drawn on and erased from the surface of amorphous powders in the quartz plate, showing excellent reversibility and recyclability. The samples could completely turn orange and fill up the entire groove when no mask was used. Moreover, the reversible transformation of crystalline and amorphous forms can be realized by means of recrystallization and rapid vacuum rotary evaporation. Thus, an interconvertible and rewritable optical information storage material could be accomplished by a simple control of the aggregated state of the solids.

3. Conclusions

In summary, a new triphenylethylene derivative, TrPE*o*PO, has been designed and successfully synthesized. The samples showed great changes in the luminescent and photochromic properties in two aggregated states. Further characterization *via* TGA, DSC, and PXRD have demonstrated that the samples underwent phase transition from crystalline to amorphous forms. Therefore, the on/off states of photochromism can be realized by the manipulation of the aggregated state of the same compound. Based on the distinct photochromic properties of the crystalline and amorphous forms, the different and convertible properties in information storage were demonstrated. This work has thus provided a new strategy for the design of switchable photochromic materials through controlling the degree of crystallinity of the aggregated solid sample. It is expected that the design principles can be further extended to similar photochromic systems to deeply understand the different properties between crystalline and amorphous states.

Author contributions

All the experiments were conducted by Mingyao Shen, Cheng Huang, Yuxin Xiao, and Rongjuan Huang with the supervision of Tao Yu. Vonika Ka-Man Au assisted in the manuscript revisions. All authors participated in the discussion and revised the manuscript.

Conflicts of interest

There are no conflicts to declare.

Acknowledgements

The authors gratefully acknowledge the financial support from the NSF of China (62275217), the Fundamental Research Funds for the Central Universities, Key Research and Development Program of Shaanxi Province (2020GXLH-Z-010), Chongqing Science and Technology Fund (cstc2020jcyj-msxmX0931), Guangdong Basic and Applied Basic Research Foundation (2021A1515010633), Natural Science Basic Research Program of Shaanxi Province (2022JQ-583), and Ningbo Natural Science Foundation (202003N4060, 20221JCGY010492). V. K.-M. A. acknowledges support by the Early Career Scheme (ECS) from the Research Grants Council of the Hong Kong Special Administrative Region, P. R. China (EdUHK 28300220).

References

1 N. M. W. Wu, M. Ng and V. W.-W. Yam, *Angew. Chem., Int. Ed.*, 2019, **58**, 3027–3031.
2 I. Yonekawa, K. Mutoh, Y. Kobayashi and J. Abe, *J. Am. Chem. Soc.*, 2018, **140**, 1091–1097.
3 L. Huang, L. Liu, X. Li, H. Hu, M. Chen, Q. Yang, Z. Ma and X. Jia, *Angew. Chem., Int. Ed.*, 2019, **58**, 16445–16450.
4 B. R. Donovan, V. M. Matavulj, S. K. Ahn, T. Guin and T. J. White, *Adv. Mater.*, 2019, **31**, e1805750.
5 W. Shen, B. Du, H. Zhuo and S. Chen, *Chem. Eng. J.*, 2022, **428**, 132609.
6 Z. Wang, J. Liu, K. Yi, P. Chen, Y. Zhu, D. Tian and B. Chu, *Chem. Eng. J.*, 2023, **455**, 140693.
7 D. M. Wu, M. L. Solomon, G. V. Naik, A. Garcia-Etxarri, M. Lawrence, A. Salleo and J. A. Dionne, *Adv. Mater.*, 2018, **30**, 1793012.
8 H. Bouas-Laurent and H. Dürr, *Pure Appl. Chem.*, 2001, **73**, 639–665.
9 H. Tian and S. Yang, *Chem. Soc. Rev.*, 2004, **33**, 85–97.
10 M. Irie, T. Fulcaminato, K. Matsuda and S. Kobatake, *Chem. Rev.*, 2014, **114**, 12174–12277.
11 J. Fritsche, *C. R. Acad. Sci.*, 1867, **69**, 1035–1037.
12 M. Irie, *Chem. Rev.*, 2000, **100**, 1685–1716.
13 J. Zhang, Q. Zou and H. Tian, *Adv. Mater.*, 2013, **25**, 378–399.
14 F. Stricker, D. M. Sanchez, U. Raucci, N. D. Dolinski, M. S. Zayas, J. Meisner, C. J. Hawker, T. J. Martínez and J. Read de Alaniz, *Nat. Chem.*, 2022, **14**, 942–948.
15 G. Huang, Q. Xia, W. Huang, J. Tian, Z. He, B. S. Li and B. Z. Tang, *Angew. Chem., Int. Ed.*, 2019, **58**, 17814–17819.
16 J. Jiang, P. Zhang, L. Liu, Y. Li, Y. Zhan, T. Wu, H. Xie, C. Zhang, J. Cui and J. Chen, *Chem. Eng. J.*, 2021, **425**, 131557.
17 H. Ju, C. N. Zhu, H. Wang, Z. A. Page, Z. L. Wu, J. L. Sessler and F. Huang, *Adv. Mater.*, 2022, **34**, e2108163.
18 B. Wu, X. Xu, Y. Tang, X. Han and G. Wang, *Adv. Opt. Mater.*, 2021, **9**, 2101266.
19 D. Li, Z. Feng, Y. Han, C. Chen, Q.-W. Zhang and Y. Tian, *Adv. Sci.*, 2022, **9**, e2104790.
20 S. Kawata and Y. Kawata, *Chem. Rev.*, 2000, **100**, 1777–1788.
21 L. Sun, B. Wang, G. Xing, C. Liang, W. Ma and S. Yang, *Chem. Eng. J.*, 2022, **455**, 140752.
22 H. Zhao, Y. Cun, X. Bai, D. Xiao, J. Qiu, Z. Song, J. Liao and Z. Yang, *ACS Energy Lett.*, 2022, **7**, 2060–2069.
23 A. Natansohn and P. Rochon, *Chem. Rev.*, 2002, **102**, 4139–4175.
24 L. N. Lameijer, S. Budzak, N. A. Simeth, M. J. Hansen, B. L. Feringa, D. Jacquemin and W. Szymanski, *Angew. Chem., Int. Ed.*, 2020, **59**, 21663–21670.
25 L. A. E. Müller, A. Zingg, A. Arcifa, T. Zimmermann, G. Nyström, I. Burgert and G. Siqueira, *ACS Nano*, 2022, **16**, 18210–18222.

26 S. Mo, Q. Meng, S. Wan, Z. Su, H. Yan, B. Z. Tang and M. Yin, *Adv. Funct. Mater.*, 2017, **27**, 1701210.
27 X. Le, H. Shang, S. Wu, J. Zhang, M. Liu, Y. Zheng and T. Chen, *Adv. Funct. Mater.*, 2021, **31**, 2108365.
28 Y. Ai, Y. Fei, Z. Shu, Y. Zhu, J. Liu and Y. Li, *Chem. Eng. J.*, 2022, **450**, 138390.
29 Z. Wang, Z. Ding, Y. Yang, L. Hu, W. Wu, Y. Gao, Y. Wei, X. Zhang and G. Jiang, *Chem. Eng. J.*, 2023, **457**, 141293.
30 Y. Yokoyama, *Chem. Rev.*, 2000, **100**, 1717–1739.
31 G. Tomasello, M. J. Bearpark, M. A. Robb, G. Orlandi and M. Garavelli, *Angew. Chem., Int. Ed.*, 2010, **49**, 2913–2916.
32 C. Eichler, A. Rázková, F. Müller, H. Kopacka, H. Huppertz, T. S. Hofer and H. A. Schwartz, *Chem. Mater.*, 2021, **33**, 3757–3766.
33 Y. Jiao, R. Yang, Y. Luo, L. Liu, B. Xu and W. Tian, *CCS Chem.*, 2022, **4**, 132–140.
34 D. Kitagawa, H. Nishi and S. Kobatake, *Angew. Chem., Int. Ed.*, 2013, **52**, 9320–9322.
35 W. Jeong, M. I. Khazi, D.-H. Park, Y.-S. Jung and J.-M. Kim, *Adv. Funct. Mater.*, 2016, **26**, 5230–5238.
36 G. M. Peters and J. D. Tovar, *J. Am. Chem. Soc.*, 2019, **141**, 3146–3152.
37 Z. Li, X. Liu, G. Wang, B. Li, H. Chen, H. Li and Y. Zhao, *Nat. Commun.*, 2021, **12**, 1363.
38 D. Ou, T. Yu, Z. Yang, T. Luan, Z. Mao, Y. Zhang, S. Liu, J. Xu, Z. Chi and M. R. Bryce, *Chem. Sci.*, 2016, **7**, 5302–5306.
39 T. Yu, D. Ou, L. Wang, S. Zheng, Z. Yang, Y. Zhang, Z. Chi, S. Liu, J. Xu and M. P. Aldred, *Mater. Chem. Front.*, 2017, **1**, 1900–1904.
40 L. Wang, T. Yu, Z. Xie, X. Chen, Z. Yang, Y. Zhang, M. P. Aldred and Z. Chi, *J. Mater. Chem. C*, 2018, **6**, 8832–8838.
41 L. Wang, T. Yu, Z. Xie, E. Ubba, T. Zhan, Z. Yang, Y. Zhang and Z. Chi, *RSC Adv.*, 2018, **8**, 18613–18618.
42 X. Zhang, T. Yu, C. Huang, H. Wang, M. Dong, R. Huang, Z. Xie, S. Wei and W. Huang, *J. Mater. Chem. C*, 2021, **9**, 11126–11131.
43 X. Zhang, F. Liu, B. Du, R. Huang, S. Zhang, Y. He, H. Wang, J. Cui, B. Zhang, T. Yu and W. Huang, *Research*, 2022, **2022**, 9834140.
44 Z. Yang, Z. Chi, T. Yu, X. Zhang, M. Chen, B. Xu, S. Liu, Y. Zhang and J. Xu, *J. Mater. Chem.*, 2009, **19**, 5541–5546.